Journal of Materials Chemistry C

Accepted Manuscript

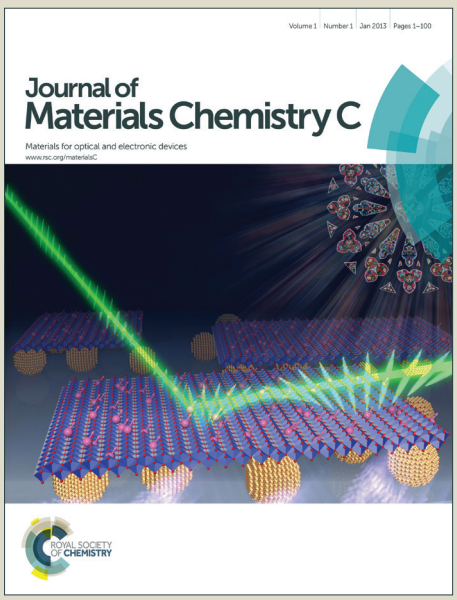

ROYAL SOCIETY OF CHEMISTRY

www.rsc.org/materialsC

Cite this: DOI: 10.1039/c0xx00000x

www.rsc.org/jmc

Paper

Low temperature and high frequency effects on polymer-stabilized blue phase liquid crystals with a large dielectric anisotropy

Fenglin Peng,[a] Yuan Chen,[a] Jiamin Yuan,[a] Haiwei Chen,[a] Shin-Tson Wu,[a*] and Yasuhiro Haseba[b]

Received (in XXX, XXX) Xth XXXXXXXXX 2014, Accepted Xth XXXXXXXXX 2014
DOI: 10.1039/b000000x

We report the low temperature and high frequency effects on polymer-stabilized blue phase liquid crystals (BPLCs) comprising of a large dielectric anisotropy nematic host. Debye dielectric relaxation sets a practical limit even the device operation temperature is still within the blue phase range. To explain these phenomena, we propose a model to describe the temperature and frequency dependent Kerr constant and obtain excellent agreement with experiment. Doping a diluter compound to the BPLC host helps to reduce viscosity, which in turn boosts the dielectric relaxation frequency and extends the low temperature operation range.

Introduction

After about one decade of extensive material research and device structure development, the major technical barriers preventing polymer-stabilized blue phase liquid crystal (PS-BPLC)[1-4] from widespread applications have been gradually overcome. The operation voltage has been reduced from 50V to 10V by employing a large dielectric anisotropy ($\Delta\varepsilon$>100) BPLC material[5,6] and implementing a device with protruded or etched electrodes.[7-10] Transmittance higher than 80% can be achieved by optimizing the refraction effect of the nonuniform fringing electric fields.[11] Hysteresis can be greatly suppressed by reducing the peak electric field near the edges of electrodes,[12] using vertical field switching,[13] adding nanoparticles[14-16], or controlling the UV exposure conditions.[17] The dawn of BPLC era seems near.

However, for a mobile display or photonic device, low temperature and high frequency operations are critical issues, especially for outdoor applications or color sequential displays using red, green and blue LEDs.[18,19] Generally speaking, the ultimate low temperature operation of a BPLC device is limited by its phase transition temperature, but in this paper we find that Debye relaxation of these large $\Delta\varepsilon$ BPLC materials sets another practical limit. Due to submillisecond gray-to-gray response time,[6,20] BPLC is ideally suited for color sequential displays. By eliminating spatial color filters, both optical efficiency and resolution density can be tripled. However, to achieve field sequential colors without seeing annoying color breakup, the required frame rate should be tripled. For example, if a spatial color-filter-based LC device is operated at 120 Hz, then the temporal color-sequential LC should be operated at 360 Hz or higher. For a large $\Delta\varepsilon$ BPLC, its Debye relaxation frequency is as low as 1.3 kHz.[6,21] Therefore, if the driving frequency gets close to the Debye relaxation frequency of the BPLC, then the Kerr constant would decrease dramatically, which in turn demands a very high operation voltage. This sets another practical limit from the viewpoint of device operation.

[a]College of Optics and Photonics, University of Central Florida, Orlando, Florida, USA. E-mail: swu@ucf.edu; Fax: +1 407-823-6880; Tel: +1 407-823-4763; [b]JNC Petrochemical Corporation, Ichihara Research Center, Ichihara, Chiba 290-8551, Japan.

In this paper, we report the low temperature and high frequency operation limits of BPLC devices. To correlate the electro-optic properties of BPLC with its LC host, we propose a physical model to describe the temperature and frequency dependent Kerr constant. The model fits well with our experimental data. To increase Debye relaxation frequency, we dope a diluter compound to the BPLC host, which greatly extends the low temperature and high frequency operation limits.

Experiment and results

In experiment, we prepared two BPLC samples employing JC-BP06N and JC-BP07N (from JNC) as LC hosts. The dielectric anisotropy at low frequency limit of JC-BP06N is 648, which is almost twice of JC-BP07N ($\Delta\varepsilon$~332). The BPLC precursors are comprised of 88.17 wt% LC host (JC-BP06N or JC-BP07N), 2.92 wt% chiral dopant R5011 (from HCCH, China), 8.70 wt% monomers (5.24 wt. % RM257 from Merck and 3.46 wt. % TMPTA (1,1, 1-Trimethylolpropane Triacrylate, from Sigma Aldrich)) and 0.21 wt% photoinitiator. These samples were filled into two in-plane-switching (IPS) cells whose electrode width is 8 μm, electrode gap is 12 μm, and cell gap is 7.34 μm. The IPS cells were coated with a thin indium tin oxide (ITO) film, but without any surface alignment layer. Both cells were cooled to BP-I phase and cured by an UV light with wavelength λ~365 nm and intensity ~2mW/cm^2 for 30 min. After UV curing, the PS-BPLC cells were quite clear because their Bragg reflections were in the UV region. For convenience, we call these two cells as PSBP-06 and PSBP-07. Next, both cells were placed on a Linkam heating stage controlled by a temperature programme (Linkam TMS94). We measured the voltage-dependent transmittance (VT) by sandwiching the heating stage between two crossed polarizers. A He-Ne laser (λ=633nm) was used as probing beam and the transmitted light was focused by a lens, so that different diffraction orders can be collected by the detector.[22]

When a LC cell is subject to an external voltage, the LC directors respond to the root-mean-square voltage (V_{rms}). In a thin-film-transistor (TFT) LCD, the driving waveform is square waves. But for studying frequency effect, sinusoidal wave is preferred because a square wave contains multiple Fourier

frequency components. Therefore, we first compare the difference between these two driving waveforms. We measured the VT curves of PSBP-06 and PSBP-07 at room temperature (RT=22°C) and several frequencies: *f*=120 Hz, 240 Hz, 480 Hz, 720 Hz and 1 kHz (both sinusoidal wave and square-wave AC voltage). It is known that under the same frequency, the root-mean-square voltage of a sine-wave is $\sqrt{2}$ larger than that of a square-wave.

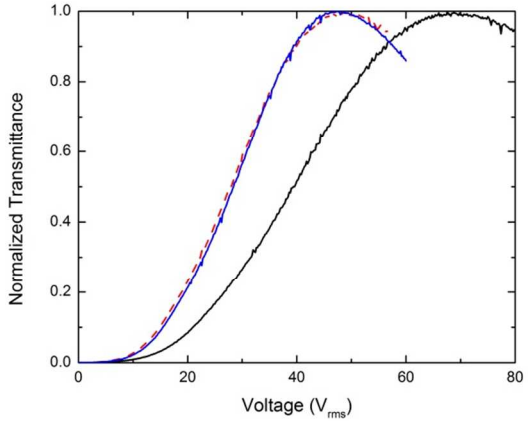

Fig. 1 Measured VT curves of PSBP-07 at *f*=480 Hz, λ=633 nm, and RT. Black curve: sine waves, blue curve: square waves, and dashed lines: black curve divided by $\sqrt{2}$.

Figure 1 shows the measured VT curves of PSBP-07 at *f*=480 Hz and λ=633 nm. The blue and black curves represent the data with square-wave and sine-wave voltages, respectively. If we divide the data points of black curve by $\sqrt{2}$, the dotted red curve overlaps with the blue curve reasonably well. Similar results are found at other frequencies and PSBP-06. Therefore, the VT curves for square waves and sine waves are consistent except their magnitude is different by a factor of $\sqrt{2}$. To simulate TFT operation, from here on we will use square-wave RMS voltage, unless otherwise mentioned.

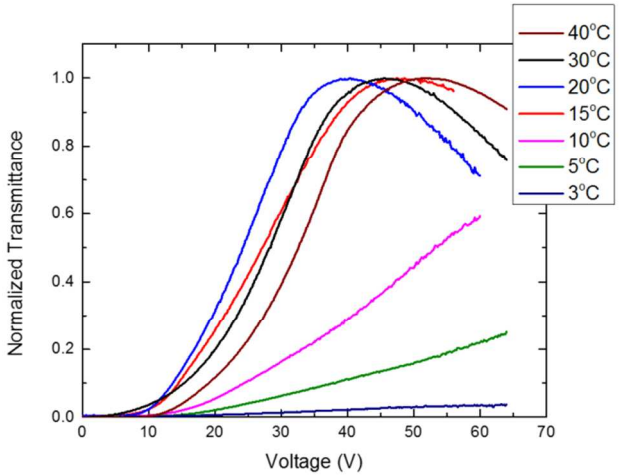

Fig. 2 Measured VT curves of PSBP-06 at the specified temperatures. *f*=480 Hz and λ=633 nm.

Next, we studied the temperature effects. Figure 2 shows the normalized VT curves of PSBP-06 measured from 40°C to 0°C at *f*=480 Hz. As the temperature (*T*) decreases, the VT curves shift leftward first and then rightward, indicating V_{on} bounces back at low temperatures. The lowest V_{on} occurs at ~20°C. As the temperature drops to 3°C, which is still above the melting point of the PSBP-06 (T_{mp}= −2°C), the transmittance stays below 5% (normalized to the peak transmittance at 60Hz under the same temperature) even the applied voltage has reached 65V_{rms}. Therefore, this imposes a practical low temperature operation limit for PSBP-06. Similar phenomenon was also observed for PSBP-07. We will further discuss this temperature limit later.

Physical mechanisms

We fit each VT curve for both cells with extended Kerr effect model[23] and plot the obtained K values in Fig. 3. In an isotropic state (left side), i.e., $T>T_c$ (clearing point), Kerr constant vanishes ($K\approx0$). As the temperature decreases from T_c, *K* increases linearly with ~*1/T*, gradually reaching a maximum, and then declines steeply. Let us call the temperature where maximum *K* occurs as optimal operation temperature, T_{op}. In the $T_c<T<T_{op}$ region, our results agree well with the model published by Rao et al [24] and Tian et al,[25] but the sharp plunge of Kerr constant when $T_{op}<T$ has not been reported previously. From Fig. 3, T_{op} depends on the BPLC material and frequency.

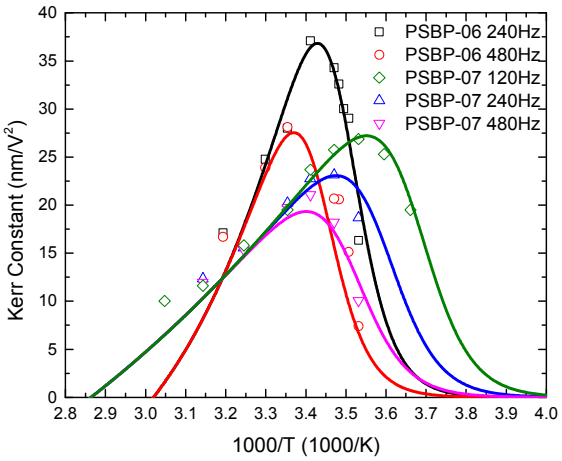

Fig. 3 Temperature dependent Kerr constants of PSBP-06 at *f*=240 Hz , 480 Hz and PSBP-07 at *f*=120 Hz, 240 Hz and 480 Hz separately. Lines represent fitting curves with Eq. (9).

To better understand the observed phenomena, we analyze the temperature and frequency effects on Kerr constant. Based on Gerber's model,[26] *K* is governed by the birefringence (Δ*n*), average elastic constant (*k*), Δε and pitch length (*P*) of the chiral LC host as:

$$K \sim \frac{\Delta n \varepsilon_o \Delta \varepsilon P^2}{k_B \lambda (2\pi)^2} \quad (1)$$

Here Δ*n*, *k*, and Δε are all temperature dependent, as described by the following relations:[22,27,28]

$$\Delta n \sim \Delta n_o S, \quad (2)$$

$$\Delta\varepsilon \sim S exp(E_1/k_B T), \quad (3)$$

$$k \sim S^2, \quad (4)$$

$$S = (1 - T/T_{cn})^{\beta}, \quad (5)$$

where *S* denotes the order parameter, Δn_o is the extrapolated birefringence at *T*=0K, E_1 is a parameter related to dipole moment, k_B is the Boltzmann constant, T_{cn} is the clearing point of the nematic host and β is a material constant. On the other hand, pitch length (P) is not sensitive to the temperature.[29] Substituting Eqs. (2), (3) and (4) into Eq. (1), we find that $K \sim exp(E_1/k_B T)$. Generally speaking, as the temperature increases *K* decreases.

From Eq. (1), the frequency effect of K originates from $\Delta\varepsilon$ because the remaining parameters are all independent of frequency in the low frequency region. Based on Debye relaxation model, $\Delta\varepsilon$ has following form:[30]

$$\Delta\varepsilon = \Delta\varepsilon_\infty + \frac{\Delta\varepsilon_o - \Delta\varepsilon_\infty}{1+(f/f_r)^2}, \quad (6)$$

where $\Delta\varepsilon_\infty$ and $\Delta\varepsilon_o$ are the dielectric anisotropy at high and low frequency limits respectively, f is the operation frequency, and f_r is the relaxation frequency. For a low viscosity nematic LC host, its f_r is usually over 100 kHz, which is much higher than the intended operation frequency (e.g., 120Hz–960Hz) of the LC device. As a result, the f/f_r term in Eq. (6) can be neglected and $\Delta\varepsilon \approx \Delta\varepsilon_o$, which is insensitive to the frequency. However for a large $\Delta\varepsilon$ BPLC, the bulky molecules cannot follow the electric field in the high frequency region. The Debye relaxation frequency is usually in the 1-2 kHz region. Thus, the f/f_r term in Eq. (6) becomes significant. As a result, $\Delta\varepsilon$ (or Kerr constant) is strongly dependent on the frequency.

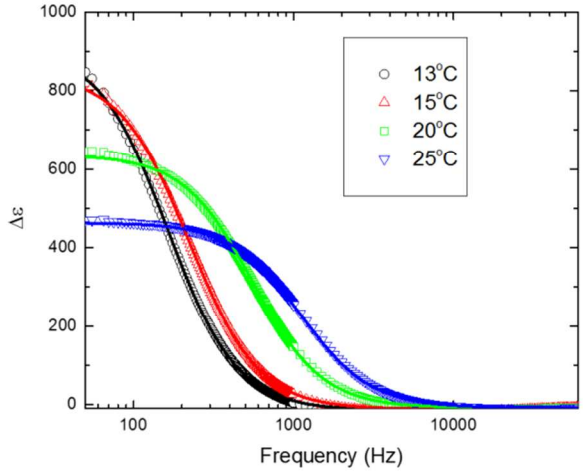

Fig. 4 Frequency dependent $\Delta\varepsilon$ of JC-BP06N at the four specified temperatures. Dots are measured data and lines are fittings with Eq. (6).

In experiment, we measured the capacitance of a homogeneous cell and a homeotropic cell using an HP-4274 multi-frequency LCR meter (sine waves) to determine the $\Delta\varepsilon$ of JC-BP06N and JC-BP07N at different temperatures.[27] Figure 4 depicts the measured $\Delta\varepsilon$ (dots) and fitting curve (solid lines) with Eq. (6) for JC-BP06N. Through fittings, f_r at each temperature is obtained. Results indicate that f_r decreases exponentially with T as:[31]

$$f_r = f_0 \cdot \exp(-E_2/k_B T), \quad (7)$$

here E_2 is the activation energy of molecular rotation and f_0 is a proportionality constant. From Eqs. (6) and (7), once f gets close to f_r, $\Delta\varepsilon$ decreases as T decreases because the ratio of f/f_r increases. As Fig. 4 shows, at 480 Hz $\Delta\varepsilon$ decreases by ~2X as T decreases from 20°C to 13°C. This explains well why V_{on} 'bounces back' as the temperature decreases [Fig. (2)]. Substituting Eqs. (3), (6) and (7) to Eq. (1), Kerr constant can be expressed as:

$$K \sim A \cdot \frac{\exp(E_1/k_B T)}{1+(f/f_r)^2} = A \cdot \frac{\exp(E_1/k_B T)}{1+[(f/f_0)\cdot\exp(E_2/k_B T)]^2}, \quad (8)$$

where A is a proportionality constant. However, when the temperature approaches T_c both Δn and $\Delta\varepsilon$ vanish, so does Kerr constant (at least dramatically decreased). To satisfy this boundary condition, we modify Eq. (8) as following:

$$K = A \cdot \frac{\exp\left[\frac{E_1}{k_B}\left(\frac{1}{T}-\frac{1}{T_C}\right)\right]-1}{1+[(f/f_0)\cdot\exp(E_2/k_B T)]^2}. \quad (9)$$

We fitted K at various temperatures with Eq. (9) for both PSBP-06 and PSBP-07. Good agreement is obtained as depicted in Fig. 3. Eq. (9) involves 4 unknowns, but f_0 and E_2 can be found by fitting the relaxation frequency, as Eq. (7) indicates. Through fitting the temperature dependent Kerr constant at a given frequency, we can obtain A and E_1. The fitting parameters are listed below. For PSBP-06, f_0=9.76x10^{18} Hz, E_1=281.0 meV, A=16.54 nm/V^2, E_2=945.1 meV, and for PSBP-07, f_0=4.80x10^{15} Hz, E_1=74.8 meV, A=37.65 nm/V^2, and E_2=736.1 meV.

In principle, we can derive the analytical form of optimal operation temperature (T_{op}) by solving $\frac{\partial K}{\partial T} = 0$, but it is too complicated to present it here. Generally, T_{op} is governed by several parameters listed in Eq. (9), such as frequency, relaxation frequency, and temperature, etc. From Fig. 2, the T_{op} of PSBP-06 at 240Hz and 480Hz occurs at 18.8°C and 22.5°C, respectively. Ideally, we would like to design a BPLC with its T_{op} (or highest Kerr constant) located at the intended operation frequency and temperature. Therefore, we investigated the frequency effect on T_{op} in more detail.

Figure 5 depicts the temperature dependent Kerr constant at different frequencies for two PSBP composites: PSBP-06 and BPLC-R1. The latter has a smaller Kerr constant because its LC host has a smaller $\Delta\varepsilon$ (~50), but its viscosity is also much lower than that of JC-BP06N. The f_r of the BPLC-R1 host is ~15 kHz at 25°C, which is ~10X higher than that of JC-BP06N. For the two BPLC samples shown in Fig. 5, the RGB curves (representing low, medium and high frequencies for each sample) overlap in the high temperature region, which means their Kerr constant is proportional to 1/T, but is quite insensitive to the frequency. This can be explained as follows. In the high temperature region, the BPLC has a lower viscosity so that its relaxation frequency is higher [Eq. (7)]. From Eq. (8), when $f_r >> f$ the frequency part can be ignored and K is inert to the frequency. As the temperature decreases (or $1/T$ increases), f_r decreases exponentially [Eq. (7)]. The blue curve (whose f is closer to f_r) bends down first due to the dramatically reduced $\Delta\varepsilon$ [Fig. 4]. As a result, its maximum Kerr constant is smaller, which leads to a higher operation voltage. For the green and red curves, their corresponding frequency is lower so that their peak Kerr constant and bending over phenomenon occur at a lower temperature, as Fig. 5 depicts.

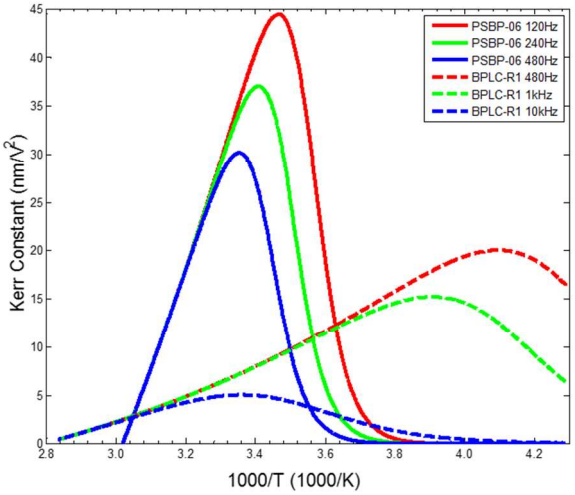

Fig. 5 Temperature dependent Kerr constant of PSBP-06 (f_r ~1.2 kHz) and BPLC-R1 (f_r ~15 kHz) at the specified frequencies. λ=633 nm.

For a given BPLC, its T_{op} increases as the frequency increases. Let us illustrate this using PSBP-06 as an example. In Fig. 5, as the frequency increases from 120 Hz to 480 Hz, the T_{op} increases gradually from 15.0°C to 22.5°C, but in the meantime Kerr constant decreases from 44.4nm/V^2 to 30.1nm/V^2. If the relaxation frequency of a BPLC is too high, then its T_{op} might shift outside the intended operation temperature range. Let us take BPLC-R1 as an example: at 480Hz its T_{op} occurs at -30°C, as Fig. 5 shows. At such a low operation temperature, the viscosity of BPLC would increase dramatically. If we want to shift T_{op} to room temperature, then the operation frequency should be increased to ~10 kHz, which would increase the power consumption dramatically. An optimal relaxation frequency should be in the 2-3 kHz range.

Diluter effect

Melting point sets the ultimate low temperature operation limit for a BPLC device. However, in this study we find another factor which limits the practical applications. Even the temperature is still above the melting point of a blue phase, the dramatic plunge of $\Delta\varepsilon$ makes the device difficult to operate, which seriously limits the usefulness of the device. Let us take PSBP-06 as an example. As the temperature decreases from 25°C to 5°C, the transmittance remains so low even the voltage has reached 65V$_{rms}$ [Fig. 2] and the decay time increases exponentially to 17ms. These problems could hinder the BPLC application in low temperatures. The abrupt decrease in Kerr constant is because the relaxation frequency is too low.

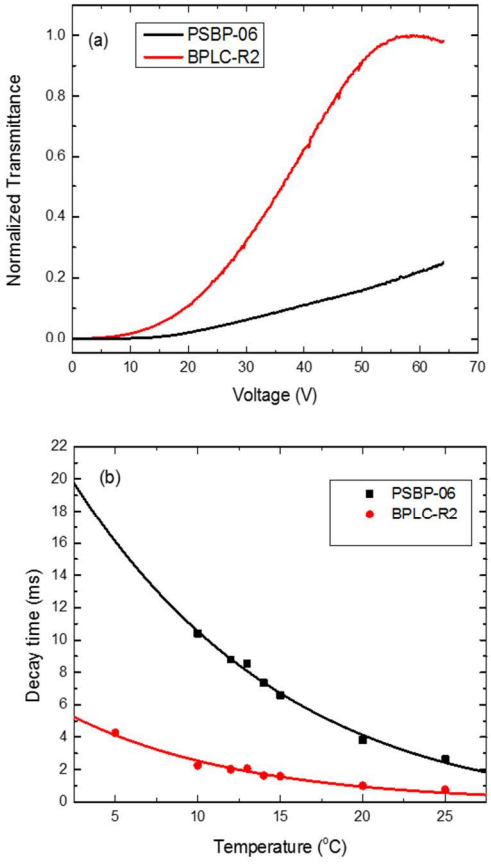

Fig. 6 (a) Measured VT curves of PSBP-06 and BPLC-R2 at 5°C with f=480 Hz and λ=633 nm; (b) Temperature dependent response time of PSBP-06 and BPLC-R2. Dots are measured data and solid lines represent fittings with Eq. (7) of Ref. 5.

To raise the relaxation frequency, doping a diluter compound has been proven to be quite effective.[32] The relaxation frequency f_r is proportional to the average molecular length (l) and viscosity η as $f_r \sim \frac{1}{\eta l^3}$.[33] Doping a low molecular weight, short-chain and low viscosity diluter to a bulky BPLC host would increase the relaxation frequency noticeably. In experiment, we doped 13 wt% 5CC3 [4-pentyl-4'-propyl-1,1'-bi(cyclohexyl)] into JC-BP06N host, which shifts f_r from 1.1 kHz to 4.85 kHz at 25°C. We call the new mixture as BPLC-R2. Although the V_{on} of BPLC-R2 is somewhat higher than that of PSBP-06 at 25°C, its performance in the low temperature region is much better than that of PSBP-06. Figure 6(a) depicts the measured VT curves and Fig. 6(b) shows the measured response time at 5°C. With diluter, both V_{on} and decay time are decreased significantly. Therefore, a good diluter helps to maintain the high performance of BPLC in the low temperature region.

Conclusions

We have developed a physical model to correlate the temperature and frequency effects on the Kerr constant of BPLC materials. The model fits very well with the experimental data. Based on the model, we find that for a given BPLC material and frequency, there exists an optimal operation temperature where the Kerr constant has a maximum value, or V_{on} is the lowest. Although the melting point of a BPLC sets its ultimate operation limit, we found another practical limit which originates from the Debye relaxation of dielectric anisotropy at low temperatures. By doping a diluter to a BPLC host helps to extend the low temperature operation limit.

Acknowledgements

The authors are indebted to Industrial Technology Research Institute (ITRI), Taiwan, for the financial support, and Yifan Liu and Jing Yan for helpful discussions.

References and Notes:

1. H. Kikuchi, M. Yokota, Y. Hisakado, H. Yang, and T. Kajiyama, *Nat. Mater*., 2002, **1**, 64.
2. Y. Hisakado, H. Kikuchi, T. Nagamura, and T. Kajiyama, *Avd. Mater.* , 2005, **17**, 96.
3. J. Yan and S. T. Wu, *Opt. Mater. Express*, 2011, **1**, 1527.
4. J. Yan, L. Rao, M. Jiao, Y. Li, H. C. Cheng, and S. T. Wu, *J. Mater. Chem.*, 2011, **21**, 7870.
5. L. Rao, J. Yan, S. T. Wu, S. Yamamoto, and Y. Haseba, *Appl. Phys. Lett.*, 2011, **98**, 081109
6. Y. Chen, D. Xu, S. T. Wu, S. Yamamoto, and Y. Haseba, *Appl. Phys. Lett.*, 2013, **102**,141116
7. M. Jiao, Y. Li, and S. T. Wu, *Appl. Phys. Lett.*, 2010, **96**, 011102
8. L. Rao, Z. Ge, and S. T. Wu, *J. Disp. Technol.*, 2010, **6**, 115.
9. S. Yoon, M. Kim, M. S. Kim, B. G. Kang, M. K. Kim, A. K. Srivastava, S. H. Lee, Z. Ge, L. Rao, S. Gauza, and S. T. Wu, *Liq. Cryst.*, 2010, **37**, 201
10. M. Kim, M. S. Kim, B. G. Kang, M. K. Kim, S. Yoon, S. H. Lee, Z. Ge, L. Rao, S. Gauza, and S. T. Wu, *J. Phys. D: Appl. Phys,* 2009, **42**, 235502.
11. D. Xu, Y. Chen, Y. Liu, and S. T. Wu, *Opt. Express*, 2013, **21**, 24721.
12. L.Rao, J.Yan, S. T.Wu, Y.C.Lai, Y.H.Chiu, H.Y.Chen, C.C.Liang, C.M.Wu, P.J.Hsieh, S.H.Liu and K.L.Cheng, *J. Disp. Technol.*, 2011, **7**, 627.
13. H. C. Cheng, J. Yan, T. Ishinabe, and S. T. Wu, *Appl. Phys. Lett.*, 2011, **98**, 261102
14. L. Wang, W. He, X. Xiao, M. Wang, M. Wang, P. Yang, Z. Zhou, H. Yang, H. Yu, and Y. Lu, *J. Mater. Chem.*, 2012, **22**, 19629.

15. L. Wang, W. He, X. Xiao, Q. Yang, B. Li, P. Yang, and H. Yang, *J. Mater. Chem.*, 2012, **22**, 2383.
16. L. Wang, W. He, Q. Wang, M. Yu, X. Xiao, Y. Zhang, M. Ellahi, D. Zhao, H. Yang, and L. Guo, *J. Mater. Chem. C*, 2013, **1**, 6526.
17. T. N. Oo, T. Mizunuma, Y. Nagano, H. Ma, Y. Ogawa, Y. Haseba, H. Higuchi, Y. Okumura, and H. Kikuchi, *Opt. Mater. Express*, 2011, **1**, 1502.
18. S. Gauza, X. Zhu, W. Piecek, R. Dabrowski, and S. T. Wu, *J. Disp. Technol.*, 2007, **3**, 250.
19. M. Kobayashi, A. Yoshida, and Y. Yoshida, *SID Int. Symp. Digest Tech. Papers*, 2010, **41**, 1434.
20. K. M. Chen, S. Gauza, H. Xianyu, and S. T. Wu, *J. Disp. Technol*., 2010, **6**, 49.
21. Y. Li, Y. Chen, J. Sun, S. T. Wu, S. H. Liu, P. J. Hsieh, K. L. Cheng, and J. W. Shiu, *Appl. Phys. Lett*., 2011, **99**, 181126
22. J. Yan, Y. Chen, S. T. Wu, and X. Song, *J. Disp. Technol*., 2013, **9**, 24.
23. J. Yan, H. C. Cheng, S. Gauza, Y. Li, M. Jiao, L. Rao, and S. T. Wu, *Appl. Phys. Lett.*, 2010, **96**, 071105
24. L. Rao, J. Yan, and S.-T. Wu, *J. Soc. Inf. Disp*, 2010, **18**, 954.
25. L. Tian, J. W. Goodby, V. Görtz, and H. F. Gleeson, *Liq. Cryst.,* 2013, **40**, 1446.
26. P. R. Gerber, *Mol. Cryst. Liq. Cryst.*, 1985, **116**, 197.
27. S. T. Wu and C. S. Wu, *Phys. Rev. A*, 1990, **42**, 2219.
28. S. T. Wu, *Phys. Rev. A*, 1986, **33**, 1270.
29. F. Zhang and D. K. Yang, *Liq. Cryst*., 2002, **29**, 1497.
30. H. Xianyu, S. T. Wu, and C. L. Lin, *Liq. Cryst.*, 2009, **36**, 717.
31. M. Schadt, *J. Chem. Phys*., 1972, **56**, 1494.
32. Y. Chen, J. Yan, M. Schadt, S. H. Liu, K. L. Cheng, J. W. Shiu, and S. T. Wu, *J. Disp. Technol*., 2013, **9**, 592.
33. L.M.Blinov, *Electro-optical and magneto-optical properties of liquid crystals* (Wiley, 1983)